

Toward energy-efficient microgrids under summer peak electrical demand integrating solar dish Stirling heat engine and diesel unit

Farkhondeh Jabari^{1,2}, Morteza Nazari-Heris^{1,3}, Behnam Mohammadi-Ivatloo^{1*}, Somayeh Asadi³, Mehdi Abapour¹

¹ Faculty of Electrical and Computer Engineering, University of Tabriz, Tabriz, Iran

² Department of Power System Operation and Planning, Niroo Research Institute (NRI), Shahrak Ghods, Tehran, Iran

³ Department of Architectural Engineering, Pennsylvania University, USA

*Corresponding author: bmohammadi@tabrizu.ac.ir

Manuscript received 26 January, 2020; revised 21 February, 2020; accepted 01 March, 2020. Paper no. JEMT- 2001-1226.

Abstract: The environmental air pollution according to greenhouse gas emissions and significant demand for electrical energy and water due to the growing population of the world can be mentioned as main challenges all around the world. The current study proposes a new structure for energy-efficient microgrids to deal with on-peak electrical energy load in summer days. Two ancillary services are considered in the proposed structure including solar Stirling engine and diesel plant for decreasing the successive outages of interconnected energy network in extremely hot weather status and eliminating massive blackouts. Such services are effective solutions to provide load and minimize the whole energy procurement cost as production-side management strategies. The objective of the proposed model is to minimize the fuel cost of the diesel plant and the cost of generated electricity by the local power network considering technical limitations of the combined diesel-Stirling electricity supply system. The optimal employment of solar-based Stirling cycle and diesel engine in providing summer peak power load are evaluated in terms of economic-environmental aspects by applying the model on a test case microgrid, which verifies high performance of the model.

Keywords: Solar dish Stirling heat engine, diesel generation unit, energy-saving, peak load procurement.

<http://dx.doi.org/10.22109/jemt.2020.217435.1226>

1. Introduction

The global concerns on air pollution due to greenhouse gas emissions and increasing energy and water demands considering the rising population of the world have made significant challenges for many countries. It is estimated that buildings account for almost 40% of primary energy and 36% of emissions of greenhouse gases [1]. Renewable energy resources based microgrids can provide energy demand close to consumers without transmission and distribution infrastructures. This cause considerable mitigation in transmission and distribution costs and power losses. The integration of renewable energies with traditional generation facilities reduces negative environmental effects of fossil fuels (ozone depletion, pollution, and acid rains). Reliability and intermittency of renewables are two significant drawbacks. Atmospheric and geographical conditions make a significant effect on the efficiency of solar, wind, tidal, etc. based microgrids.

Therefore, incorporation of more reliable power generation units such as diesel engines overcomes uncertainties associated with their daily and seasonal variations. Also, the design of zero energy buildings (ZEBs) as a promising solution for the environmental and economic issues in the world is an important subject in the developed countries because of its effectiveness in reducing electrical energy and water consumption [2, 3]. Because electrical energy is generally produced by using fossil fuels which one is the main contributor to greenhouse gas emissions, the design of ZEBs will have a positive influence on reducing the pollutant gases emitted to the environment. Additionally, the design of the ZEBs will benefit us in terms of electricity bills since the allocation of renewable energy sources such as photovoltaic cells installed on the roof, glasses and ground, and wind turbines will be sufficient to supply the required electrical energy of the building. Also, the water management methodologies and water sustainability features are effective in decreasing the utilization of water sources [4]. Such methodologies and features are effective in increasing the water

sources for future communities and decrease water costs [5, 6]. In recent decades, researchers have tried to propose different methodologies to overcome environmental and economic issues associated with the performance of residential buildings over the life cycle mainly by focusing on environmental-friendly and efficient designs of ZEBs. Such buildings have been introduced as a sustainable solution to decrease the building demand and pollution emissions by using renewable energy sources and energy storage systems [7] which will result in less electricity consumption in comparison with traditional buildings.

Researchers have made significant efforts for improving the efficiency and design of ZEBs using various methodologies and strategies. An energy-based approach for ZEBs has been introduced in [8] to simplify the decision-making procedure, where the advantages of this method for residential's heat comfort level and energy efficiency indexes are investigated for a case study. The authors have aimed to determine an optimal and near ZEB solution based on the European energy performance of buildings directive (EPBD-recast 2010) in (EPBD-recast 2010), which is applied to a case study in Finland, and the effect of design-variable integrations have been evaluated. A new multi-story residential ZEB has been presented in Denmark in [9] for investigating the index of energy efficiency and renewable resources, where various configurations of a photovoltaic system and heating equipment have been studied. The authors have studied phase change materials (PCMs) as a passive approach to be integrated to near ZEBs for absorbing extra heat during the day and releasing the heat stored during the night [10]. In [11], the authors have discussed the reconstruction and re-use of an exhibitively energy-efficient building, which is known as a case study of a building with high efficiency. A combination of thermal energy storage in nearly ZEB is introduced in [12] for application of PCM into storage tank, where enough building heating and cooling is made by increment of on-site utilization of self-supplied solar power and integration of PV, power storage, heat pump, heat storage, and energy management system of the building. The energy performance of a near ZEB with PV cells considering electrical and heat storage systems is analyzed in [13], where rule-based control methodologies are applied for simulating the operation of storage systems. An energy-exergy-environment-based structure is proposed in [14] for the heat pump refrigeration cycle to apply in large residential buildings. The introduced design in this reference employed a solar Stirling engine [15] to provide the electricity required by the heat pump. Also, an adiabatically compressed air energy storage system is used for storing the excess of power at off-peak time intervals and consumes it at on-peak time intervals. In [16], a ZEB based on photovoltaic thermal technology and a ground source heat pump has been proposed, which has employed a geothermal heat pump for supplying domestic hot water and heating load of the building.

On the other side, different methods have been proposed for improving the economic indexes of microgrids. The authors have studied optimal power flow in electrical energy systems considering multiple-fuel options and prohibited operating zones in [17] using a solver-friendly mixed integer nonlinear programming, which has been verified on both small-scale and large-scale systems. In [18], hybrid price-based demand response has been proposed for the day-ahead scheduling of residential microgrids, where the uncertain nature associated with plants and load are investigated, and the effect of the proposed demand response program on the load profile has been evaluated. The application of fuel-cell to store hydrogen and CHP plants for simultaneous power and heat generation in micro-grids has been studied in [19] considering uncertainties of the grid including the load and power market. A robust model for the operation of microgrids has been proposed in [20] to deal with the worst-case condition of the system against power market price uncertainty, where the profit of the system is increased considering

heat and power resources. An optimization model for optimal operation of an integrated heat and power network is investigated in [21] concerning uncertainty issues of electrical load, where demand response programs are considered for smoothing the load pattern. The authors have presented a novel optimization strategy for operation of reconfigurable microgrids with the ability of islanding from the main grid in [22], where a chance-constrained formulation is proposed to minimize the whole operation cost of the system. The authors have proposed a smart transactive energy model in [23] for home microgrids with the capability of collaborating with each other in the energy market, where the optimal operation of energy sources in the studied system is attained by allocating profit with the formation of the coalition. A hierarchical energy management system for multiple home energy hubs in the neighborhood grid has been introduced in [24], which aims to maximize the profit of the system and shave the upstream network on-peak demand by appropriate power generation/storage decision-making method. In [25], a stochastic risk-constrained scheduling model is proposed for autonomous microgrids considering reliability and economic analysis, where the maximization of the expected profit of the microgrid is the main objective of the proposed model. The authors have studied optimal energy management of micro-grids with hydro and thermal generation sources in [26] by applying robust optimization model to increase the benefit of the micro-grid when selling power to the market. The integration of power to gas (P2G) system to coupled gas and power systems has been evaluated in [27] through an economic analysis of the system considering price-responsive shiftable demands, where the P2G has been proven to be effective for increasing dispatch of wind power in the power system.

Comparing to the reviewed publications in the area of ZEBs and the operation of micro-grids, this study aims to propose a model for handling on-peak demand on summer days by introducing a novel approach. The current research presents a new methodology to supply the on-peak demand for electrical energy during summer days. Two ancillary services consisting of solar Stirling engine and diesel system are included in the proposed model as shown in Fig. 1 in the proposed model. These services are promising ways to supply demand and decrease total energy procurement costs as supply-side management approaches. The proposed model is solved by implementing COUENNE tool in the General Algebraic Modeling System (GAMS) software considering a series of technical limitations of combined diesel-Stirling units. The effectiveness of the proposed model is evaluated by analyzing the simulation results on a test case in terms of economic and environmental aspects. The outcome of this research will help the power system operators in providing summer on-peak energy demands with advantages of both the economic daily saving of the system and decreasing the maximum energy load of the main electrical energy network. The main contributions of this study can be listed as follows:

- Investigating the optimal application of a solar-based Stirling cycle and diesel engine in supplying summer peak power demand.
- Reducing the successive outages of the integrated energy system in extremely hot weather conditions and removing massive blackouts.
- Minimizing the fuel cost of the diesel unit and the produced power cost of the local power system.
- Studying energy management of the system by considering both economic and environmental aspects.

This paper is organized as follows: the problem formulation has been given in Section 2. The case study for the proposed ZEB model and simulation results have been provided in Section 3. Finally, the conclusion of the paper is given in Section 4.

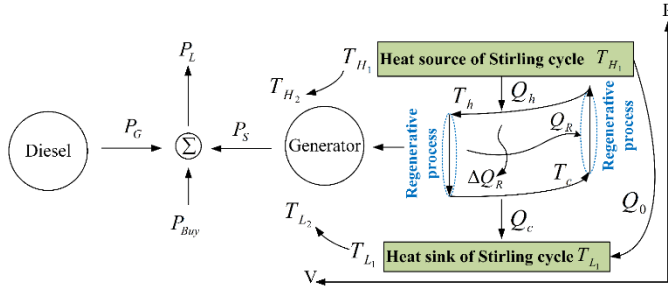


Fig. 1. The proposed scheme for the studied microgrid

2. Problem formulation

Equation 1 can be used for determining the usable heat gain of dish collector concerning the losses during conducting, convecting and radiating processes [28].

$$q_u = IA_{app}\eta_0 - A_{rec}[h(T_{H_{ave}} - T_0) + \varepsilon\delta(T_{H_{ave}}^4 - T_0^4)] \quad (1)$$

where, I and A_{app} are the respective indicators of direct solar flux intensity and collector aperture area. Moreover, η_0 and h are the collectors optical efficiency and heat transmission coefficient during the conduction/convection practice. The area and average of absorber temperature are A_{rec} and $T_{H_{ave}}$. Also, T_0 , ε and δ are ambient temperature, collector emissivity factor and Stefan's constant.

The thermal efficiency of the dish collector η_s is computed as (2) [29]:

$$\eta_s = \frac{q_u}{IA_{app}} = \eta_0 - \frac{1}{IC}[h(T_{H_{ave}} - T_0) + \varepsilon\delta(T_{H_{ave}}^4 - T_0^4)] \quad (2)$$

2.1 Regenerative heat losses

It is worth to mention that a bounded heat transmission exists in the regenerative heat transfer that can be formulated as [30]:

$$Q_r = nC_v\varepsilon_R(T_h - T_c) \quad (3)$$

where ΔQ_r is the heat loss in two-cycle regenerative operations. Based on (3), we can write [30]:

$$\Delta Q_r = nC_v(1 - \varepsilon_R)(T_h - T_c) \quad (4)$$

where, n and C_v are the respective indicators of mass and heat capacity of working fluid in mole in regenerative operations. Also, ε_r is the regenerator productivity, and T_h and T_c are the respective temperatures of working fluid in hot and cold places. We cannot neglect the time duration of the regenerative process in comparison with two isothermal processes concerning the irreversible impact of finite-rate heat transition [31]. To compute it, we can assume that working fluid is a function of time duration as (5) [31]:

$$\frac{dT}{dt} = \pm M_i \quad (5)$$

The ratio constant M is a function of a property of regenerative substance known. Moreover, \pm sign is used for determining heating ($i = 1$) and cooling ($i = 2$) processes [31].

$$t_3 = \frac{T_1 - T_2}{M_1} \quad (6)$$

$$t_4 = \frac{T_1 - T_2}{M_2} \quad (7)$$

2.2 Source heat released and sink heat absorbed

The heat released/absorbed of the interplay between working fluid (Q_h) with a heat source for released heat and with a heat sink (Q_c) for absorbed heat, can be attained using equations (8) and (9) [32]:

$$Q_h = nRT_h \text{Ln}\lambda + nC_v(1 - \varepsilon_R)(T_h - T_c) \quad (8)$$

$$Q_c = nRT_c \text{Ln}\lambda + nC_v(1 - \varepsilon_R)(T_h - T_c) \quad (9)$$

Also, we have:

$$Q_h = [C_H\varepsilon_H(T_{H_1} - T_h) + \xi C_H\varepsilon_H(T_{H_1}^4 - T_h^4)]t_h \quad (10)$$

$$Q_c = C_L\varepsilon_L(T_c - T_{L_1})t_l \quad (11)$$

Where, C_H/C_L shows heat capacitance rate for heat source/sink for external fluids.

$$\varepsilon_H = 1 - e^{-N_H} \quad (12)$$

$$\varepsilon_L = 1 - e^{-N_L} \quad (13)$$

Where, ε_H and ε_L are the productivity of high/low-temperature heat exchangers. Also, N_L and N_H define cyclic periods calculated by $N_L = U_L A_L / C_L, N_H = U_H A_H / C_H$. The cyclic interval t is as (14) based on (3)-(11).

$$t = \frac{nRT_h \text{Ln}\lambda + nC_v(1 - \varepsilon_R)(T_h - T_c)}{C_H\varepsilon_H(T_{H_1} - T_h) + \xi C_H\varepsilon_H(T_{H_1}^4 - T_h^4)} + \frac{nRT_c \text{Ln}\lambda + nC_v(1 - \varepsilon_R)(T_h - T_c)}{C_L\varepsilon_L(T_c - T_{L_1})} + \left(\frac{1}{M_1} + \frac{1}{M_2}\right)(T_h - T_c) \quad (14)$$

2.3 Heat losses between source to sink

Losses of heat bridging between sink and source are directly based on the mean temperature difference between sink and source and cycle time, which is as [32]:

$$Q_o = K_o(T_{H_{ave}} - T_{L_{ave}})t_{\text{cycle}} \quad (15)$$

$$T_{H_{ave}} = \frac{T_{H_1} + T_{H_2}}{2} \quad (15a)$$

$$T_{L_{ave}} = \frac{T_{L_1} + T_{L_2}}{2} \quad (15b)$$

Moreover, we have [33]:

$$T_{H_2} = (1 - \varepsilon_H)T_{H_1} + \varepsilon_H T_h \quad (15c)$$

$$T_{L_2} = (1 - \varepsilon_L)T_{L_1} + \varepsilon_L T_c \quad (15d)$$

So, based on (15a)-(15d), we have:

$$Q_o = \frac{K_o}{2}[(2 - \varepsilon_H)T_{H_1} - (2 - \varepsilon_L)T_{L_1} + (\varepsilon_H T_h - \varepsilon_L T_c)]t_{\text{cycle}} \quad (16)$$

The sheer released/absorbed heat from/by the source/sink, which is indicated by Q_H/Q_L can be defined as:

$$Q_H = Q_h + Q_o \quad (17)$$

$$Q_L = Q_c + Q_o \quad (18)$$

The output electricity, heat efficiency, and supply of engine concerning the cyclic time of the Stirling engine can be computed as:

$$P = \frac{W}{t} = \frac{Q_H - Q_L}{t} \quad (19)$$

$$\eta_i = \frac{Q_H - Q_L}{Q_H} \quad (20)$$

$$\sigma = \frac{1}{t} \left(\frac{Q_L}{T_{L_{ave}}} - \frac{Q_H}{T_{H_{ave}}} \right) \quad (21)$$

Considering (3)-(14), we can have (19) and (20):

$$P_{\text{Stirling}} = nR(T_h - T_c) \text{Ln}\lambda / \left(\frac{nRT_h \text{Ln}\lambda + nC_v(1 - \varepsilon_R)(T_h - T_c)}{C_H\varepsilon_H(T_{H_1} - T_h) + \xi C_H\varepsilon_H(T_{H_1}^4 - T_h^4)} + \frac{nRT_c \text{Ln}\lambda + nC_v(1 - \varepsilon_R)(T_h - T_c)}{C_L\varepsilon_L(T_c - T_{L_1})} + \left(\frac{1}{M_1} + \frac{1}{M_2}\right)(T_h - T_c) \right) \quad (22)$$

$$\eta_i = nR(T_h - T_c) \text{Ln}\lambda / (nRT_h \text{Ln}\lambda + nC_v(1 - \varepsilon_R)(T_h - T_c) + \frac{K_o}{2}[(2 - \varepsilon_H)T_{H_1} - (2 - \varepsilon_L)T_{L_1} + (\varepsilon_H T_h - \varepsilon_L T_c)]t_{\text{cycle}}) \quad (23)$$

The lower limit of heat efficiency of total solar-dish Stirling engine can

be attained based on thermal efficiencies of collector and Stirling engine, as [28]:

$$\eta_m = \eta_s \eta_t \quad (24)$$

2.4 Model of diesel engine

A diesel engine is employed in this study as a second back up power source. A minimum output for diesel power as 30% of diesel nominal power is considered for the operation of the diesel to eliminate the operation of the diesel at high load. The diesel engine will run at the minimum bound when the power needed is lower than the minimum amount, while the extra generated power will be sold to the power grid. It will be shut off if no power is needed. The hourly fuel consumption of the diesel generator, F_G , is defined as (25) [34].

$$F_G = B_G \times P_{DC} + A_G \times P_G \quad (25)$$

Also, P_{DC} and P_G are the respective indicators of nominal power and hourly power output of the generator. A_G and B_G are the fuel curve slope and the fuel curve intercept coefficient, respectively.

2.5 Objective function and constraints

The objective function of the system, which is the minimization of the fuel cost of diesel engine and the cost of power purchased from the upper grid, can be written as (26). The technical limits and the operational constraints of the proposed microgrid are fulfilled considering (27)-(32) in the optimization process.

$$OF = \sum_{t=1}^{24} \lambda_e^t P_{buy}^t + \sum_{t=1}^{24} \lambda_{fuel} F_G^t \quad (26)$$

In which, OF is the objective function, λ_e^t and P_{buy}^t are the hourly power price and the power purchased from the main grid, and λ_{fuel} is the diesel fuel cost, which is almost constant 1.24 \$/Liter. Also, the fuel consumption of the diesel is indicated by F_G^t .

$$P_L^t \leq P_G^t + P_S^t + P_{buy}^t \quad (27)$$

$$P_G^t \leq P_{DC} \quad (28)$$

$$\eta_m \geq 0.3 \quad (29)$$

$$\sum_{t=1}^{24} P_{buy}^t \leq 0 \quad (30)$$

$$800 \leq T_h \leq 1050 \quad (31)$$

$$400 \leq T_c \leq 510 \quad (32)$$

Where, P_{DC} is the nominal power of a diesel.

3. Numerical result and discussions

As mentioned in Section 1, the use of solar Stirling engine and diesel generation units leads to a significant reduction of the electrical power purchased from the local power system, because increasing the rate of direct solar flux intensity and ambient air temperature increases both energy demand and output Stirling power. Therefore, optimal short-term coordination of solar dish Stirling heat engine and a diesel generator is proposed to procure on-peak electricity demand in summer. GAMS is used to simulate the non-linear programming problem (1)-(32) and minimize the total fuel cost of the diesel generation unit and the cost of power purchased from the upstream energy network over the 24-h study horizon. For this purpose, the maximum power consumption of the benchmark microgrid during the hottest summer day is considered in the optimization problem, as shown in Fig. 2 [14]. It is assumed that the direct solar flux intensity, I , changes as shown in Fig. 3 [35]. Moreover, other constant factors related to the solar dish Stirling engine [32] and diesel unit [34] are reported in Table 1. Figure 4 demonstrates the hourly changes in the electricity price during the sample summer day [36].

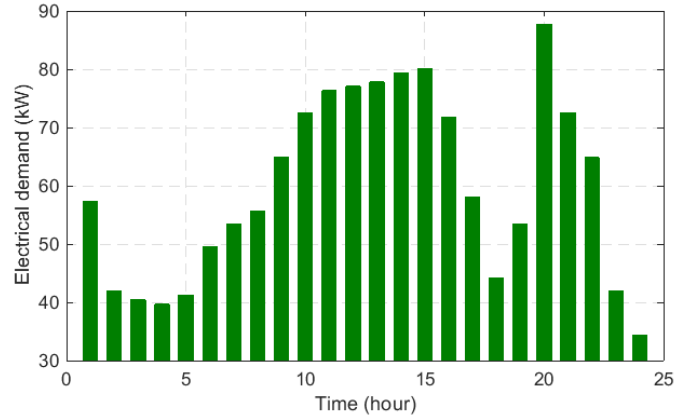


Fig. 2. The electrical power consumption of the residential microgrid [14]

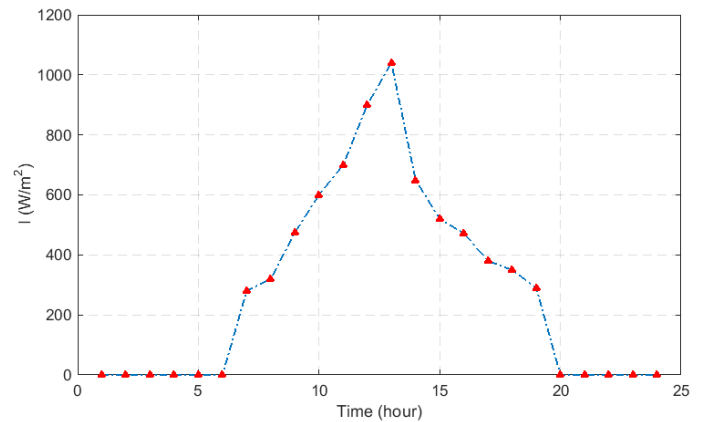


Fig. 3. Daily variations of direct solar flux intensity, I [35]

Table 1. The technical specifications of the solar Stirling engine [32] and the diesel generating unit [34]

λ	n	$R(\text{J} \cdot \text{mol}^{-1} \cdot \text{K}^{-1})$	$T_{H_1}(\text{K})$	$T_L(\text{K})$	$C_v(\text{J} \cdot \text{mol}^{-1} \cdot \text{K}^{-1})$
5	1	4.3	1300	290	15
$P_{DC}(\text{kW})$	ε_H	ε_L	ε_R	C_H, C_L	$\lambda_{fuel}(\text{\$/Liter}^{-1})$
15	0.8	0.8	0.9	1800	1.24

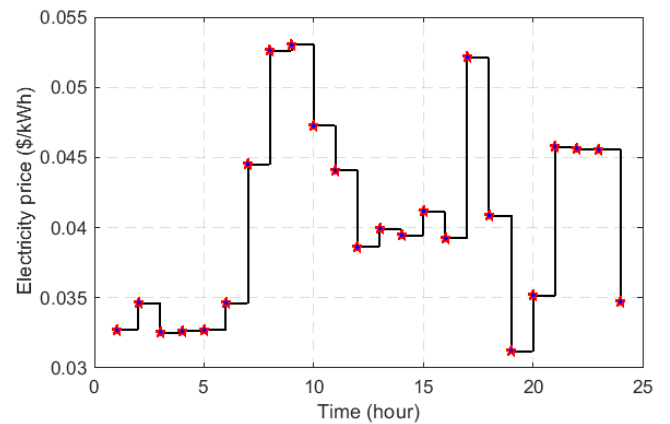


Fig. 4. The hourly energy tariffs over the study period [36]

The decision variables of the optimization problem are considered as follows: The value of the power purchased from the local power grid, P_{buy}^t , the output power of the solar Stirling cycle, P_S^t , the power generation of the diesel unit, P_G^t , the working fluid temperatures in the cold space and heat

source, T_h and T_c , the cyclic interval t , the thermal efficiency of the dish collector, η_s , the thermal efficiency of the Stirling engine, η_l , the maximum thermal efficiency of the solar dish Stirling heat engine, η_m , the secondary temperature of the working fluid in the heat source, T_{H_2} , the average temperature of the working fluid in the hot space, $T_{H_{ave}}$, the secondary temperature of the working fluid in the cold space, T_{L_2} , and the average temperature of the working fluid in the heat sink, $T_{L_{ave}}$, are selected as the decision variables of the optimal short-term scheduling problem. The convex over and under envelopes for nonlinear estimation (COUENNE) tool of the GAMS software is employed for finding the best operating point of the Stirling-diesel hybrid power generation microgrid. The optimum values of the decision variables related to the solar dish Stirling cycle during the sun radiation period (from $t = 7$ to $t = 19$) are presented in Table 2.

Table 2. The decision variables related to the Stirling heat engine during the solar irradiation time interval

t	T_h	T_c	η_s	η_l	η_m	T_{H_2}	$T_{H_{ave}}$	T_{L_2}	$T_{L_{ave}}$	P'_S
7	1015	410	0.574	0.523	0.3	1072	1186	386	338	98.96
8	1042	457	0.605	0.496	0.3	1093	1196	424	357	106.72
9	1037	510	0.703	0.454	0.319	1089	1194	466	378	109.35
10	1037	510	0.744	0.454	0.338	1089	1194	466	378	109.35
11	1037	510	0.766	0.454	0.348	1089	1194	466	378	109.35
12	1037	510	0.796	0.454	0.362	1089	1194	466	378	109.35
13	1037	510	0.81	0.454	0.368	1089	1194	466	378	109.35
14	1037	510	0.756	0.454	0.343	1089	1194	466	378	109.35
15	1037	510	0.72	0.454	0.327	1089	1194	466	378	109.35
16	1037	510	0.7	0.454	0.319	1089	1194	466	378	109.35
17	1040	504	0.652	0.46	0.3	1092	1196	461	375	109.26
18	1043	484	0.63	0.476	0.3	1094	1197	445	367	108.6
19	1027	423	0.581	0.517	0.3	1081	1190	396	343	101.86

As expected from relation (2), the thermal efficiency of the dish collector η_s increases while increasing the direct solar flux intensity, I . This causes the improvement of the heat efficiency of the entire solar Stirling cycle, η_m , as formulated by (2), (23) and (24). It is obvious that increasing of thermal efficiency of solar Stirling engine causes its output power production increases and vice versa. It is obvious from Fig. 3 and Table 2 that if the direct solar flux intensity increases, the maximum thermal efficiency of the entire solar dish Stirling cycle will increase while improving its power output. Moreover, the solar Stirling engine is able to produce 109.35 kW power as its capacity from $t = 10$ to $t = 16$. According to Fig. 2, the peak electrical demand of the benchmark microgrid is 87.745 kW, which occurs at hour 20. Meanwhile, the generation capacity of the diesel unit is assumed to be 15 kW. Therefore, the diesel generating unit cannot supply the energy consumption of the test system. In the same manner, there is no sufficient solar irradiation from $t = 1$ to $t = 6$ and $t = 20$ to $t = 24$. Hence, the output power of the solar Stirling engine is equal to zero within these time intervals. Therefore, the Stirling engine cannot support the electrical load at these periods. Accordingly, the diesel unit and the solar dish Stirling engine are optimally co-scheduled during the sample day. As shown in Figs. 5 and 6, if the

diesel unit consumes 4.912 Liters fuel to produce 15 kW at hours 8 and 9 and 2.635 Liters to generate 5.746 kW in time 17, the objective cost function will reduce from \$58.8 to \$43.3. In other words, without the application of solar Stirling engine and diesel producer, the total electrical demand of the test system will be supported by the local power grid that causes \$58.8 daily energy procurement cost. When these units have co-operated for satisfying demand, the diesel unit participates in the load procurement process at hours 8, 9, and 17. Besides, the Stirling engine is able to produce the surplus power for selling to the local power grid during the solar irradiation period. Therefore, the value of the power purchased from the main energy network is negative that indicates the power sold to the upstream grid and obtaining \$3.8 over the study horizon ($\sum_{t=1}^{24} \lambda_e^t P_{buy}^t = \3.8), as illustrated in Fig. 7. The optimum daily fuel cost of the diesel unit is \$47.2 ($\sum_{t=1}^{24} \lambda_{fuel}^t F_G^t = \47.2). This results in $\$58.8 + \$3.8 - \$47.2 = \15.4 cost saving in the daily operation cost of this microgrid. The calculation time of the optimization problem in all cases is less than 2 seconds. Integration of solar dish Stirling heat engine with diesel generator not only make it possible to generate power at night and when solar irradiation is insufficient, but also causes significant cost saving over summer days. Moreover, it will be possible to procure some of the on-peak electrical demand in the summer and flat load curve. As future trends, uncertainties associated with solar direct flux intensity, electricity rates, and demand can be studied using stochastic, probabilistic, info-gap modes, game theory, etc. Moreover, thermal energy storage systems can be integrated with a solar Stirling engine based microgrid to improve its efficiency and reliability and make it possible to produce power at all hours.

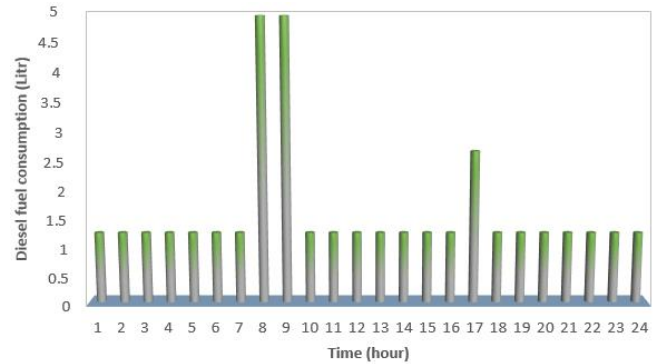


Fig. 5. The fuel consumption of the diesel unit in the sample summer day

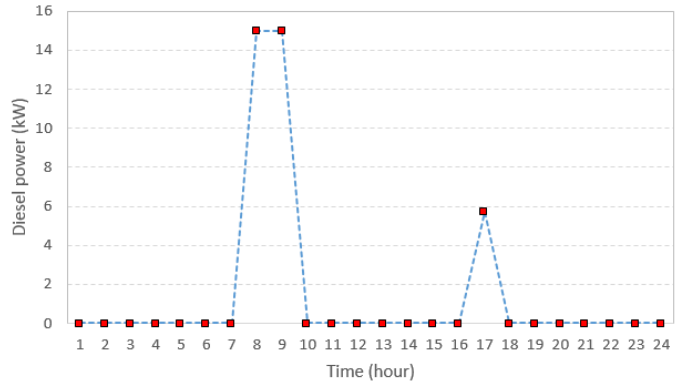


Fig. 6. The electrical power produced by the diesel generator

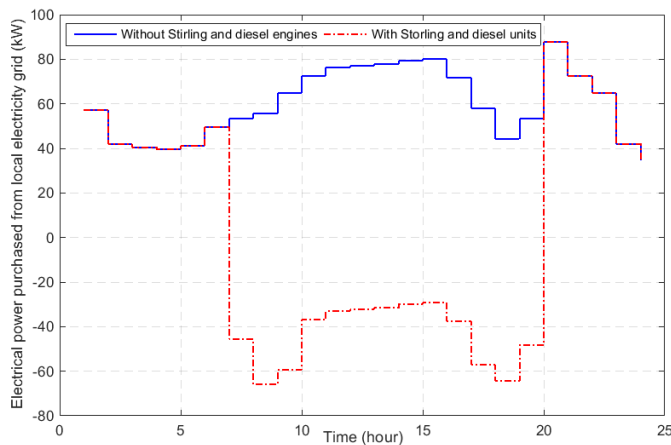


Fig. 7. The electrical power purchased (+)/sold (-) from/to the local energy network

4. Conclusions and future trends

This paper presented a novel framework for supplying on-peak electrical demand in summer. To reduce successive outages of the interconnected electricity system in extremely hot weather conditions and prevent massive blackouts, two ancillary services including solar Stirling engine and diesel unit are proposed for supplying demand and minimizing total energy procurement cost as generation-side management strategies. The proposed method aimed at minimizing the fuel consumption cost of the diesel unit and the cost of electrical power procured by the local energy grid considering the technical limits of the diesel-Stirling integrated power generation system. It is proved that the optimal application of a solar-driven Stirling cycle and diesel engine in supplying summer peak energy requirement of test microgrid not only resulted in \$15.4 economic daily saving for the owner but also reduced the maximum energy demand of the main power system. Moreover, the increasing pattern of ambient air temperature and direct solar flux intensity caused a significant improvement in the output power of the Stirling engine as well as its maximum thermal efficiency. In other words, the coefficient of performance of the diesel-Stirling engines-based power generation system increased as the solar irradiation increased and vice versa, which revealed the economic-environmental benefits of the presented network.

Acknowledgments

This work has been supported under the International Cooperation in Applied Research Development (ICARD) program by the Center for International Scientific Studies & Collaboration (CISSC), Iran.

References

- [1] Eurostat, "Final energy consumption by sector, Available at: <http://epp.eurostat.ec.europa.eu/portal/page/portal/statistics/search/database> ." 2014.
- [2] A. Karji, A. Woldesenbet, M. Khanzadi, and M. Tafazzoli, "Assessment of Social Sustainability Indicators in Mass Housing Construction: A Case Study of Mehr Housing Project," *Sustainable Cities and Society*, vol. 50, p. 101697, 2019.
- [3] S. V. Russell-Smith, M. D. Lepech, R. Fruchter, and Y. B. Meyer, "Sustainable target value design: integrating life cycle assessment and target value design to improve building energy and environmental performance," *Journal of Cleaner Production*, vol. 88, pp. 43-51, 2015.
- [4] N. L. Poff *et al.*, "Sustainable water management under future uncertainty with eco-engineering decision scaling," *Nature Climate Change*, vol. 6, no. 1, pp. 25-34, 2016.
- [5] G. Georgiou, P. Christodoulides, S. A. Kalogirou, and G. A. Florides, "Optimal utilization of Renewable Energy Sources in nearly Zero Energy Buildings—A review," 2016.
- [6] M. Hamdy, A.-T. Nguyen, and J. L. Hensen, "A performance comparison of multi-objective optimization algorithms for solving nearly-zero-energy-building design problems," *Energy and Buildings*, vol. 121, pp. 57-71, 2016.
- [7] D. D'Agostino and L. Mazzarella, "What is a Nearly zero energy building? Overview, implementation and comparison of definitions," *Journal of Building Engineering*, vol. 21, pp. 200-212, 2019.
- [8] S. Attia, E. Gratia, A. De Herde, and J. L. Hensen, "Simulation-based decision support tool for early stages of zero-energy building design," *Energy and buildings*, vol. 49, pp. 2-15, 2012.
- [9] A. J. Marszal and P. Heiselberg, "Life cycle cost analysis of a multi-storey residential net zero energy building in Denmark," *Energy*, vol. 36, no. 9, pp. 5600-5609, 2011.
- [10] U. Stritih, V. Tyagi, R. Stropnik, H. Paksoy, F. Haghghat, and M. M. Joybari, "Integration of passive PCM technologies for net-zero energy buildings," *Sustainable cities and society*, vol. 41, pp. 286-295, 2018.
- [11] A. Brambilla, G. Salvalai, M. Imperadori, and M. M. Sesana, "Nearly zero energy building renovation: From energy efficiency to environmental efficiency, a pilot case study," *Energy and Buildings*, vol. 166, pp. 271-283, 2018.
- [12] E. Zavr and U. Stritih, "Improved thermal energy storage for nearly zero energy buildings with PCM integration," *Solar Energy*, vol. 190, pp. 420-426, 2019.
- [13] V. Gjorgievski *et al.*, "Sizing of Electrical and Thermal Storage Systems in the Nearly Zero Energy Building Environment-A Comparative Assessment," in *2019 1st International Conference on Energy Transition in the Mediterranean Area (SyNERGY MED)*, 2019, pp. 1-6: IEEE.
- [14] F. Jabari, S. Nojavan, and B. M. Ivatloo, "Designing and optimizing a novel advanced adiabatic compressed air energy storage and air source heat pump based μ -Combined Cooling, heating and power system," *Energy*, vol. 116, pp. 64-77, 2016.
- [15] Y. Bravo *et al.*, "Environmental evaluation of dish-Stirling technology for power generation," *Solar Energy*, vol. 86, no. 9, pp. 2811-2825, 2012/09/01/ 2012.
- [16] Y. Chen, A. Athienitis, and K. Galal, "Modeling, design and thermal performance of a BIPV/T system thermally coupled with a ventilated concrete slab in a low energy solar house: Part 1, BIPV/T system and house energy concept," *Solar Energy*, vol. 84, no. 11, pp. 1892-1907, 2010.
- [17] M. Pourakbari-Kasmaei, M. Lehtonen, M. Fotuhi-Firuzabad, M. Marzband, and J. R. S. Mantovani, "Optimal power flow problem considering multiple-fuel options and disjoint operating zones: A solver-friendly MINLP model," *International Journal of Electrical Power & Energy Systems*, vol. 113, pp. 45-55, 2019.
- [18] H. J. Monfared, A. Ghasemi, A. Loni, and M. Marzband, "A hybrid price-based demand response program for the residential micro-grid," *Energy*, vol. 185, pp. 274-285, 2019.
- [19] M. Nazari-Heris, S. Abapour, and B. Mohammadi-Ivatloo, "Optimal economic dispatch of FC-CHP based heat and power micro-grids," *Applied Thermal Engineering*, vol. 114, pp. 756-769, 2017.
- [20] M. Nazari-Heris, B. Mohammadi-Ivatloo, G. B. Gharehpetian, and M. Shahidehpour, "Robust short-term scheduling of integrated heat and power microgrids," *IEEE Systems Journal*, vol. 13, no. 3, pp. 3295-3303, 2018.
- [21] M. Majidi, B. Mohammadi-Ivatloo, and A. Anvari-Moghaddam, "Optimal robust operation of combined heat and power systems with demand response programs," *Applied Thermal Engineering*, vol. 149, pp. 1359-1369, 2019.
- [22] M. Hemmati, B. Mohammadi-Ivatloo, M. Abapour, and A. Anvari-Moghaddam, "Optimal Chance-Constrained Scheduling of

Reconfigurable Microgrids Considering Islanding Operation Constraints," *IEEE Systems Journal*, 2020.

[23] M. Marzband, F. Azarnejadian, M. Savaghebi, E. Pouresmaeil, J. M. Guerrero, and G. Lightbody, "Smart transactive energy framework in grid-connected multiple home microgrids under independent and coalition operations," *Renewable energy*, vol. 126, pp. 95-106, 2018.

[24] H. R. Gholinejad, A. Loni, J. Adabi, and M. Marzband, "A hierarchical energy management system for multiple home energy hubs in neighborhood grids," *Journal of Building Engineering*, vol. 28, p. 101028, 2020.

[25] M. Vahedipour-Dahraie, H. Rashidzadeh-Kermani, A. Anvari-Moghaddam, and J. M. Guerrero, "Stochastic Risk-Constrained Scheduling of Renewable-Powered Autonomous Microgrids with Demand Response Actions: Reliability and Economic Implications," *IEEE Transactions on Industry Applications*, 2019.

[26] M. Nazari-Heris, S. Madadi, and B. Mohammadi-Ivatloo, "Optimal management of hydrothermal-based micro-grids employing robust optimization method," in *Classical and recent aspects of power system optimization*: Elsevier, 2018, pp. 407-420.

[27] M. Nazari-Heris, M. A. Mirzaei, B. Mohammadi-Ivatloo, M. Marzband, and S. Asadi, "Economic-environmental effect of power to gas technology in coupled electricity and gas systems with price-responsive shiftable loads," *Journal of Cleaner Production*, vol. 244, p. 118769, 2020.

[28] L. Yaqi, H. Yaling, and W. Weiwei, "Optimization of solar-powered Stirling heat engine with finite-time thermodynamics," *Renewable energy*, vol. 36, no. 1, pp. 421-427, 2011.

[29] B. J. Kaldehi, A. Keshavarz, A. A. Safaei Pirooz, A. Batooei, and M. Ebrahimi, "Designing a micro Stirling engine for cleaner production of combined cooling heating and power in residential sector of different climates," *Journal of Cleaner Production*, vol. 154, pp. 502-516, 2017/06/15/ 2017.

[30] A. Sharma, S. K. Shukla, and K. A. Rai, "Finite time thermodynamic analysis and optimization of solar-dish Stirling heat engine with regenerative losses," *Thermal Science*, vol. 15, no. 4, pp. 995-1009, 2011.

[31] M. H. Ahmadi, S. S. G. Aghaj, and A. Nazeri, "Prediction of power in solar Stirling heat engine by using neural network based on hybrid genetic algorithm and particle swarm optimization," *Neural Computing and Applications*, vol. 22, no. 6, pp. 1141-1150, 2013.

[32] M. H. Ahmadi, A. H. Mohammadi, S. Dehghani, and M. A. Barranco-Jimenez, "Multi-objective thermodynamic-based optimization of output power of Solar Dish-Stirling engine by implementing an evolutionary algorithm," *Energy conversion and Management*, vol. 75, pp. 438-445, 2013.

[33] S. Kaushik and S. Kumar, "Finite time thermodynamic analysis of endoreversible Stirling heat engine with regenerative losses," *Energy*, vol. 25, no. 10, pp. 989-1003, 2000.

[34] A. M. Abdelshafy, H. Hassan, and J. Jurasz, "Optimal design of a grid-connected desalination plant powered by renewable energy resources using a hybrid PSO-GWO approach," *Energy conversion and management*, vol. 173, pp. 331-347, 2018.

[35] F. Jabari, M. Nazari-heris, B. Mohammadi-ivatloo, S. Asadi, and M. Abapour, "A solar dish Stirling engine combined humidification-dehumidification desalination cycle for cleaner production of cool, pure water, and power in hot and humid regions," *Sustainable Energy Technologies and Assessments*, vol. 37, p. 100642, 2020/02/01/ 2020.

[36] F. Jabari, B. Mohammadi-ivatloo, and M. Mohammadpourfard, "Robust optimal self-scheduling of potable water and power producers under uncertain electricity prices," *Applied Thermal Engineering*, vol. 162, p. 114258, 2019/11/05/ 2019.